Electrospun flexible self-standing γ-alumina fibrous membranes and their potential as high efficiency fine particulate filtration media

Yan Wang, Wei Li, Yuguo Xia, Xiuling Jiao[*] **and Dairong Chen**[*]

Novel self-standing γ-alumina fibrous membranes with good flexibility have been successfully fabricated by electrospinning technique for the first time. The γ-alumina membranes were composed of randomly arranged nanofibers with high aspect ratio and small diameter (ca. 230 nm). The γ-alumina membranes show high tensile strength (2.98 MPa) and thermal stability (up to 900 °C), which favor their applications in high temperature conditions. Furthermore, the γ-alumina membranes exhibit good filtration performance for 300 nm DOP (dioctyl phthalate) fine particulate gas filtration. The filtration efficiency is 99.848% and the pressure drop is 239.12 Pa for the membrane calcined at 700 °C with a basis weight of 9.28 g m^{-2}, and the filtration efficiency could be over 99.97% when the basis weight is over 11.36 g m^{-2}, suggesting that the γ-alumina fibrous membrane is a promising candidate for high-temperature fine particulate filtration application. This work also provides novel insight into electrospinning flexible self-standing inorganic membranes for application in separation field.

Introduction

Air pollution is a significant health hazard to humankind and it attracts much attention these years due to the rapid urbanization and industrialization.[1,2] As one of the key factors that contributes to the air pollution, the suspended particulate matter (PM) in the air has been consistently associated with atherosclerosis problem,[3] retinal microvascular changes,[4] cardiovascular disease,[5] preeclampisa,[6] and etc. Gas filtration is one of the most important routes to reduce the injury of PM through filtering the exhaust gas or air, in which the filtration performance mainly depends on the filtration material.

Recently, nonwoven fibrous membrane has been widely used in various filtration applications, and it is generally considered that the filtration performance can be improved by reducing the fiber diameter.[2,7-10] Particularly, the fibrous membranes produced by electrospinning technique exhibit excellent filtration property due to its large surface-to-volume ratio, small fiber diameter, high porosity, high permeability and

interconnected open pore structure.[7,11-16] In the past few years, large numbers of fibrous membranes fabricated by electrospinning method were applied in gas filtration. These fibrous membranes involves a wide variety of materials such as Nylon 6,[8,13] elastomeric,[7] polyacrylonitrile (PAN),[15,17] polyethylene oxide (PEO),[18] polyurethane,[19] polyamide-66[20] and polyvinyl chloride/polyurethane.[21] Besides, many related properties including the effects of face velocity and nanofiber packing density on filtration performance[18] and filtration mechanism,[19] as well as the mechanical property of the membranes[21] have been studied extensively. The results indicate that the electrospun fiber membranes have superior filtration performance comparing to the traditional filtration materials. However, in previous reports most of the investigations focused on polymer fibrous membranes, which possess low thermal stability and cannot be used in high temperature circumstance. In the actual production, the exhaust gases from metallurgy, electric power, and etc are with high temperature and contain harmful particulate, which contributes a lot to the air pollution. Thus high-temperature filtration materials are worth to be studied intensively.

Inorganic fibrous membranes possess high chemical and thermal stability and can be used under severe conditions. However, the inorganic fibrous membranes are usually fragile which limits their practical application. This is because the electrospun membranes are xerogel fibrous membranes and the calcination procedure is usually necessary to convert them into inorganic membranes. During the calcinations procedure, the solvent, organic additives, carbon and inorganic anions in the precursor were removed to form the inorganic materials. In most cases, crystallization and grain growth also occurred during the calcinations process. These easily lead to the generation of pores and the decrease of the fibers' mechanical property. Therefore, the inorganic membranes are usually fragile and could not be self-standing membranes. The self-standing inorganic membranes could only be obtained by choosing appropriate precursor, adjusting electrospinning parameters and carefully controlling the calcinations procedure. Up to now, the report on self-standing inorganic membranes is very limited. Only a few kinds of flexible inorganic membranes such as SiO_2-TiO_2 composite fibrous membrane and SiO_2 membrane have been fabricated by electrospinning.[22-24]

Among the inorganic materials, alumina is one of the most important functional materials with many

attractive properties such as high melting point, high thermal and chemical stability. Based on these characteristics, alumina has been widely studied as filtration materials.[25-28] Recently, alumina fibrous membranes have been fabricated by self-assembly of alumina nanofibers[29] or filtering a mixture of boehmite nanofiber sol and organic solvent.[30] The alumina fibers that composed these membranes were nanofibers with diameters of 2-10 nm and lengths of 200-6000 nm, which are conducive to their adsorption application but adverse to their flexibility and mechanical property. Therefore, the membranes are being used as sorbent, but not suitable for self-standing filtration media. Compared to the above methods, electrospinning technique is more suitable for the fabrication of nanofibrous membranes with good mechanical properties. The alumina fibers fabricated by electrospinning method attracts much attention in recent years. To date, various precursors such as PAN/DMF solution[31] and aluminium chloride hydroxide/poly(vinyl alcohol) solution[32] have been applied and analyzed, and different kinds of alumina fibers including transparent alumina (Al_2O_3) nanofiber,[33] ultra-fine α-Al_2O_3 fiber,[34] and mesoporous alumina fibers[35] have been fabricated by electrospinning method. However, these researches are based on single alumina fiber which is not convenient for use in practical applications. Recently, our group reported the fabrication of flexible alumina fibers by electrospinning method.[36,37] However, the tensile stress is not high enough to be used as self-standing filtration media, and there are many aspects to be improved. Therefore, the fabrication of fibrous alumina membranes as self-standing filtration media is still a great challenge.

In this work, we fabricated novel self-standing γ-alumina fibrous membranes through a simple and convenient electrospinning method. The morphology, mechanical properties, thermal stability and long-term stability of the membranes were investigated. Furthermore, the gas filtration performance of γ-alumina membranes with various calcinations temperatures and different basis weights was also studied.

Experimental section

Preparation

All materials were purchased commercially and without any further purification, which include HCOOH

(analytical grade), CH₃COOH (analytical grade), aluminum powder (analytical grade), polyethylene oxide (PEO, M_W=500000).

In a typical synthesis, 6.03 mL of HCOOH and 6.86 mL of CH₃COOH were dissolved in 17.28 mL of deionized water. Then, 1.08 g aluminum powder was added into the solution. The mixture was stirred and refluxed at 60~80 °C till the aluminum powder reacted completely. The solution was filtered to remove a small amount of residual impurities and finally a colorless transparent solution was formed. Then, 0.1 g of PEO was added into the as-obtained solution to improve the spinnability of the sol. The sol was fed through a 10.0 mL plastic syringe with a 0.9 mm inner diameter metallic needle at a speed of 2.0 mL h⁻¹. The distance between the needle and the collector was 17.0 cm, and the applied voltage was 18 kV. The humidity was controlled below 10% during the electrospinning process. The as prepared gel fiber membranes were dried at 80 °C for 24 h, and then calcined under a calcination procedure of firstly 1 °C min⁻¹ to 600 °C for 2 h and then 5 °C min⁻¹ to designed temperature for 2 h.

Characterization

The Al species in the precursor were analyzed by ²⁷Al nuclear magnetic resonance (NMR) spectroscopy using a Bruker Avance 300 (78.2 MHz) spectrometer. The morphology of the fibers was observed by a field emission scanning electron microscopy (FE-SEM, JSM-6700F) and transmission electron microscopy (TEM, JEM-1011). The thicknesses of the membranes were measured on an SEM (SH-3000, HIROX). The optical microscope image was taken by a HXD-1000TMC/LCD microscopic tester. The phase of the fiber membranes were characterized by X-ray diffraction (XRD, Rigaku D/Max 2200PC) with CuKα radiation (λ=0.15418 nm) at room temperature, and the applied tube voltage and electric current were 40 kV and 20 mA. Thermo-gravimetric and differential scanning calorimetry (TG-DSC) measurements were characterized on a Mettler Toledo SDTA851e thermo-gravimetric analyzer with a heating rate of 10 °C min⁻¹ and up to 1200 °C in air atmosphere. The mechanical properties of the membranes were tested on a tensile tester (XG-1A, Shanghai New Fiber Instrument Co., Ltd., China) with a champ distance of 5 mm and a drawing speed of 1 mm min⁻¹.

The filtration efficiency and pressure drop were tested on a TSI model 8130 automated filter tester (TSI,

Inc., MN, USA)，which could deliver charge neutralized oily DOP (Di-Octyl Phthalate) aerosols with a mass median diameter of 300 nm and a geometric standard deviation not exceeding 1.6. The DOP aerosols were fed into a filter holder and down through the filter with an inner diameter of 14 cm. The aerosol concentrations before and after filtration were measured by two solid-state laser photometers, and the pressure drop was measured by the combination of a flow meter and two electronic pressure transducers. The DOP aerosol velocities were fixed at 30 L min^{-1} and 85 L min^{-1}, respectively.

Results and discussion

Fabrication and structure of γ-alumina fibrous membranes
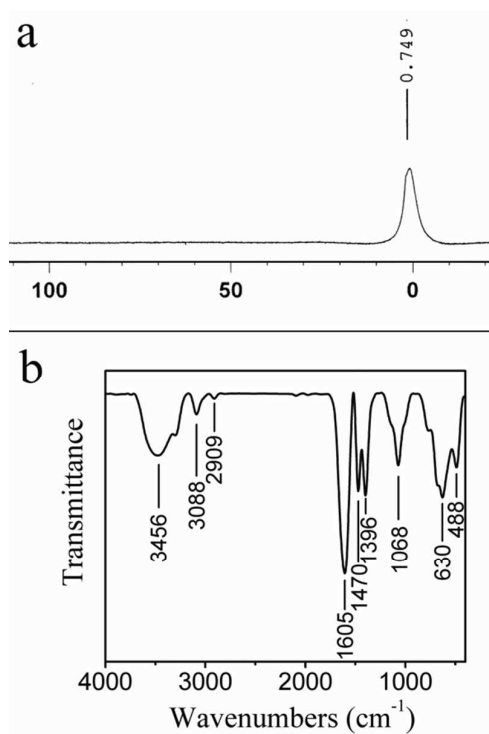
Fig. 1 ^{27}Al nuclear magnetic resonance (NMR) spectrum (a) and FT-IR spectrum of the xerogel fibers.

The alumina precursor was prepared by the reaction of aluminum powder with carboxylic acid. The amounts of aluminum powder, formic acid and acetic acid were controlled at an appropriate proportion (approximately 1:4:3 in molar ratio) to form a stable and clear solution. The status of aluminum was Al^{3+} in the final solution, which could be identified from ^{27}Al nuclear magnetic resonance (NMR) spectrum (Fig. 1). Generally, the ^{27}Al signal near 0 ppm corresponds to the aluminum ions.[38] Then a small amount of PEO

was added into the solution, which could adjust the viscosity and improve spinnability of the solution. The appropriate amount of PEO was necessary for electrospinning. If the content of PEO was less than 0.1 g, the sol was unable to be electrospun to form the alumina fibers. If overmuch PEO was added, the sol was too viscous to flow through the needle and it was not spinnable. Based on the experiments, the sol showed good electro-spinnability when the PEO amount is in the range of 0.1-0.5 g. Since the PEO will be removed during calcinations, PEO content could impact the compactness of the fibers and thus influence the tensile stress of the fibrous membranes. In the spinnable range, the less amount of PEO added in the sol, the better the alumina membranes are. Therefore, 0.1 g PEO was chosen as the optimal content. The solution was electrospun to form the xerogel fibrous membrane. During the electrospinning process, the hydroxyl and carboxyl groups connected with aluminum were further polymerized with the evaporation of the solvent to form the -Al-O-C- linked polymer, and the ambient condition was maintained at an appropriate humidity (below 15%) to control the rate of solvent evaporation. Because the acidity of formate, it is easy to react with hydroxyl groups to form the -Al-O-C- polymers with the removal of H_2O molecules:

$$Al\text{-}OOCH + HO\text{-}Al \rightarrow \text{-}Al\text{-}O\text{-}C\text{-}O\text{-}Al\text{-} + H_2O$$
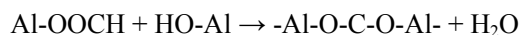
This reaction could be confirmed by the IR spectrum of the xerogel fibrous membrane. Theoretically, the Al-O-Al linkages give rise to absorptions between 945 and 990 cm^{-1}, while those of Al-O-C linkages are between 1028 and 1070 cm^{-1}.[39] At the same time, C-O-C bonds also have absorptions between 900 and 1150 cm^{-1}, which can be introduced by the additive PEO. Fig. S1 presents the IR spectrum of PEO. The strong absorptions at 1104 cm^{-1} and 955 cm^{-1} are associated to C-O-C linkage, and there are several other strong peaks such as 841 cm^{-1}, 1283 cm^{-1}, and 1349 cm^{-1} existed. However, in the IR spectrum of the xerogel fibers (Fig. 1b), only a peak at 1068 cm^{-1} is observed, which reveals that the IR absorptions for C-O-C linkage cannot be observed in the present experiment due to its small content. Therefore, the peak at 1068 cm^{-1} is ascribed to the absorption of Al-O-C linkages. As shown in Fig. 2, there are three modes for carboxylate ligands bonding to Al: monodentate, bridging and bidentate. For the monodentate configuration, there is only one oxygen atom bonded to the aluminum. In the bridging and bidentate coordination, the oxygen atoms are both bonded but on different aluminum atom for the bridging type and

on the same aluminum atom for the bidentate type. The frequency differences between v_s (COO) and v_{as} (COO) modes can be used to identify the coordination geometry of the carboxylate with metal atom.[40-42] Frequency differences for the monodentate, bridging and bidentate type are respectively of ~300 cm^{-1}, ~200 cm^{-1} and <80 cm^{-1}.[40] In this study, the absorptions at 1605 cm^{-1} and 1396 cm^{-1} respectively correspond to the asymmetrical stretching vibration and symmetrical stretching vibration of COO$^-$, which are the characteristic bands of the carboxylate. Obviously, the frequency difference between v_{as} (COO) and v_s (COO) is 209 cm^{-1}, indicating the bridge-bonding of carboxylate to two aluminum atoms. This result is similar to the previous reports about the coordination type of carboxylate bonding on alumina surface,[41,42] further indicating the occurrence of the above described reaction. Additionally, the band at 3456 cm^{-1} proved the existence of –OH. The weak bands at 3088 cm^{-1} and 2909 cm^{-1} are characteristic absorptions of carboxylic acid, indicating that a small amount of incompletely reacted carboxylic acid still exists in the xerogel fibers. The absorption at 1470 cm^{-1} is due to the antisymmetric deformation vibration of –CH$_3$, those at 630 cm^{-1} and 488 cm^{-1} are ascribed to the Al-O vibration mode.
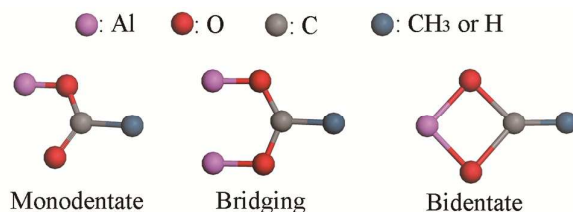
Fig. 2 Three proposed structures for carboxylate binding to aluminum atom.

Fig. 3a shows the optical image of the xerogel fibrous membranes. When the sol was electrospun, the fibrous membrane was formed on the collector immediately. The thickness of the membrane could be adjusted by differing the spinning time. The fibrous membrane can keep the original condition without any crack after several times of crimping and folding. Optical microscope and SEM image were studied to identify whether there are any crack generated after crimping and folding (Fig. S2). It can be seen that there is no crack observed in the whole membrane, and the fibers are still continuous, indicating the xerogel fibrous membrane has remarkable flexibility and bending property. Fig. 3b indicates that the xerogel fibers

have high aspect ratios with uniform diameters of ca. 330 nm. The fibers oriented randomly and thus a lot of interconnected open pores existed, which makes contribution to the permeability of the fibrous membrane. Fig. 3b's inset shows that there are raised strips on the surface of the xerogel fibers, which may be related to the rheological property of the sol precursor and the uneven moisture evaporation during electrospinning and drying process. Fig. 3c presents the TG-DSC curves of the xerogel fibrous membrane, which exhibits a total weight loss of 62.53% until 600 °C due to the decomposition of organics and removal of water. The exothermic peak from 650 to 900 °C corresponds to the transformation from amorphous alumina to γ-alumina. XRD patterns (Fig. 3d) are consistent with the TG-DSC analysis. The xerogel fibrous membranes are amorphous while the membranes calcined at 700-900 °C exhibit γ-alumina phase with characteristic peaks at 45° and 67°. The grain size of the γ-alumina fiber was approximately 10 nm, which was calculated by Debye-Scherrer formula. When the calcination temperature was up to 1000 °C, the δ-alumina and α-alumina phase appeared, and the membranes became fragile. As a result, the membranes could not be self-standing ones.
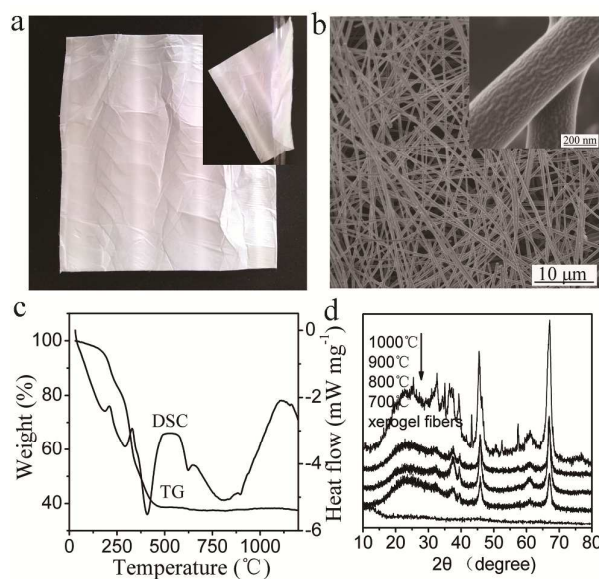
Fig. 3 Optical images (a), SEM images (b), TG-DSC curves (c) of the xerogel fibrous membrane and XRD patterns (d) of the xerogel fibrous membranes and those calcined at different temperatures.
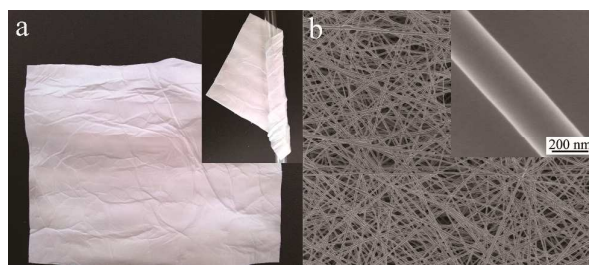
Fig. 4 Optical images (a) and SEM images (b) of the γ-alumina fibrous membrane calcined at 900 °C.

The xerogel membranes were dried intensively before calcinations. Then the membranes were firstly calcined at low temperature at a slow heating rate to reduce the generation of internal defects caused by the removal of the residual H_2O, HCOOH, CH_3COOH, PEO and other organics, then calcined at high temperature at a relative rapid heating rate to ensure the completely crystallization of γ-alumina. The morphology of the γ-alumina fibrous membrane obtained at 900 °C was shown in Fig. 4. After calcinations, the xerogel fibrous membrane transformed to γ-alumina fibrous membrane. The sizes of the fibrous membranes calcined at 700 °C, 800 °C and 900 °C shrank to 61.63%, 59.25% and 58.8% of the xerogel fibrous membrane, respectively. Fig. 4a presents the optical graphs of the calcined membranes after crimping and bending several times (inset in Fig. 4a), and there is no crack generated, indicating the good flexibility of the calcined fibrous membrane. SEM images (Fig. 4b) indicates that the γ-alumina fibers still retains high aspect ratios, and the holes formed by the randomly arranged fibers still exist. The diameter of the fibers decreases compared to the xerogel fibers and the surface of the fibers become smooth. These changes were caused by the decomposition of organics and the transformation from amorphous alumina to γ-alumina. The morphologies of other γ-alumina fibrous membrane obtained at 700 °C and 800 °C are generally the same as described above. One significant difference is that the pores in a single fiber become more patently and the average fiber diameter slightly reduces with the calcination temperature rising (Fig. 5). For the membranes calcined at 700 °C, the fibers are dense without any pores (Fig. 5a), while the pores can be observed gradually for the membranes calcined at 800 °C and 900 °C (Fig. 5b and Fig. 5c), and the average fiber diameter decreases slightly, which are respectively 250 nm, 230 nm and 200 nm for the membranes calcined at 700 °C, 800 °C and 900 °C. These changes may be caused by the gradual grain

growth of γ-alumina at high temperatures.
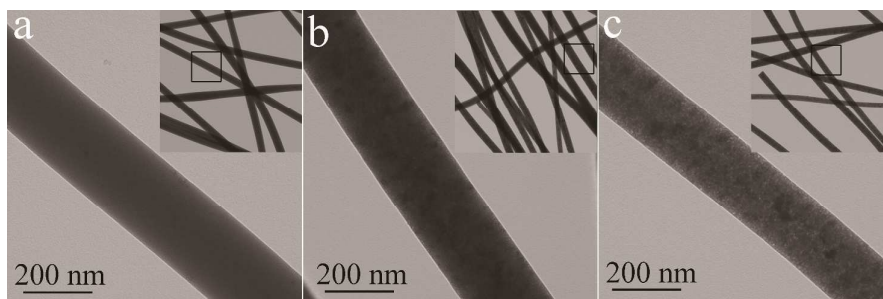
Fig. 5 TEM images of the alumina fibers calcined at 700 °C (a), 800 °C (b) and 900 °C (c).
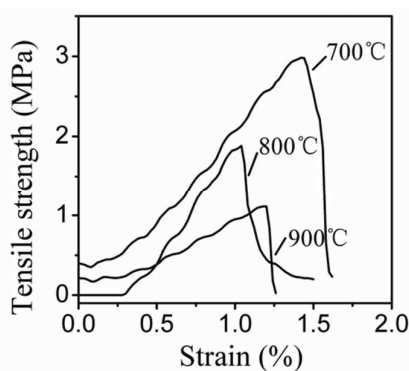
Fig. 6 Tensile stress–strain curves of γ-alumina fibrous membranes obtained at different temperatures.

The typical tensile strength-strain curves of γ-alumina fibrous membranes are presented in Fig. 6. The γ-alumina fibrous membranes obtained at 700 °C exhibited a remarkable tensile stress of 2.98 MPa and an elongation at the break value of 1.5%. The high tensile stress is attributed to the dense nature of the fibers, small fibers diameters, high aspect ratios and small grain size that composed the fibers. The high tensile stress is good for its filtration application. With the calcination temperatures raised to 800 °C and 900 °C, the tensile stress decreased to 1.88 and 1.11 MPa respectively, which may be caused by the formation of more silt pores at higher calcinations temperatures.

To identify the thermal stability of the fabricated membrane, the γ-Al_2O_3 membrane obtained at 900 °C was further calcined at 900 °C for 24 h. As shown in Fig. 7, the membrane after 24 h calcinations at high temperature is still flexible. SEM images show the fibers that compose the membrane are still continuous with uniform diameters, and the surface of the fibers is still smooth. XRD proves that the membrane still

remains the γ-Al$_2$O$_3$ structure without obvious change. The tensile stress (1.13 MPa) is almost the same as

that before calcinations (1.11 MPa). These results reveal that the membrane could keep its original status

after calcinations at high temperature, which means the γ-alumina fibrous membranes possess high thermal

stability and can be used in high temperature circumstances. Furthermore, the long-term stability of the

fabricated membrane was also investigated. Fig. S3 presents the properties of γ-Al$_2$O$_3$ membranes obtained

at 700 °C and after kept at ambient condition for eight months. The membrane is still flexible, and the fibers

are still continuous with uniform diameters and smooth surface. XRD pattern indicates the γ-Al$_2$O$_3$

structure of the membrane. The tensile stress (2.94 MPa) is almost the same as that of the original

membrane (2.98 MPa). In brief, there is no obvious change for the membrane after being kept for eight

months, indicating the good long-term stability of the fabricated membranes. The high thermal stability and

long-time stability of the membrane favor its practical application.
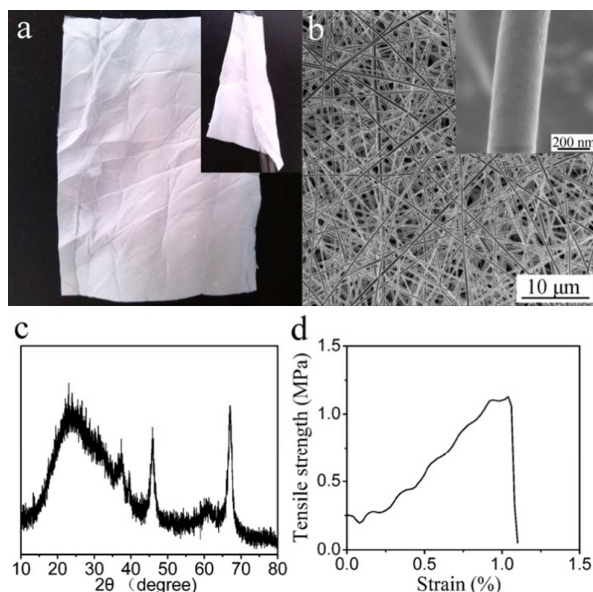
Fig. 7 Optical images (a), SEM images (b), XRD patterns (c) and tensile stress–strain curves (d) of the

membranes that obtained at 900 °C and further calcined at 900 °C for 24 h.

Evaluation of filtration performance
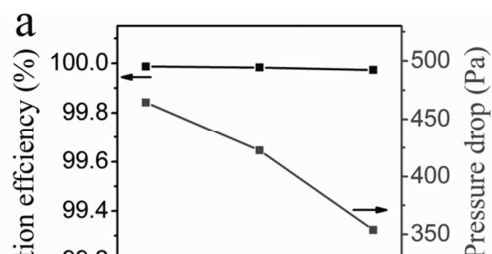
Fig. 8 Filtration performance of alumina membranes calcined at different temperatures with a similar basis weight of 15.5 g m^{-2}. (a) Filtration efficiency and pressure drop, (b) QF values.

The filtration performances of the membranes were tested by DOP method. DOP is a common aerosol for filtration test, and the method for filtration test using DOP originated in USA. This method was used for testing high efficiency particulate filter according to US military standard (MIL. STD.-282),[43] and now is an international general method to evaluate the smoke penetration and gas resistance of filters. In this work, DOP could atomize to form 300 nm liquid smoke, which could represent the fine particulate in practical application. The filtration performances toward dioctyl phthalate (DOP) with 300 nm diameter for the γ-alumina membranes calcined at different temperatures are shown in Fig. 8. Generally, the removal of sub-micron aerosol particles by fibrous membranes is primarily based on the following mechanisms: Brown diffusion, direct interception, inertial impaction, gravity force and chemical/physical or electrical attraction. The filtration efficiencies of the samples calcined at 700 °C, 800 °C, and 900 °C are 99.987%, 99.983% and 99.973%, respectively. The corresponding pressure drops are respectively 464.50 Pa, 422.53 Pa and 353.78 Pa for the samples calcined at 700°C, 800°C and 900°C. Based on the filtration efficiency and pressure

drop, the quality factor (QF) is a comprehensive parameter for comparing filtration performance of different filters, which is defined as:[44]

$$QF=[-\ln(1-\eta)]/\Delta p$$

Where η and Δp represent the filtration efficiency and pressure drop, respectively. A better filter is the one that possesses higher filtration efficiency and/or lower pressure drop, which corresponds to a higher QF value.[8,45] Fig. 8b shows the QF values of the samples that calcined at 700 °C, 800 °C, and 900° C, which are 0.01926, 0.02054 and 0.02323 Pa^{-1}, respectively. The QF indicates that filtration performance of the membrane becomes better with the calcination temperature rising. It can be seen from Fig. 8a that the filtration efficiency decreases slightly while the pressure drop decreases obviously with the calcinations temperature rising. Thus decrease of the pressure drop contributes a lot to the change of the QF value. This phenomenon may derive from the further shrinkage of the fiber diameter.
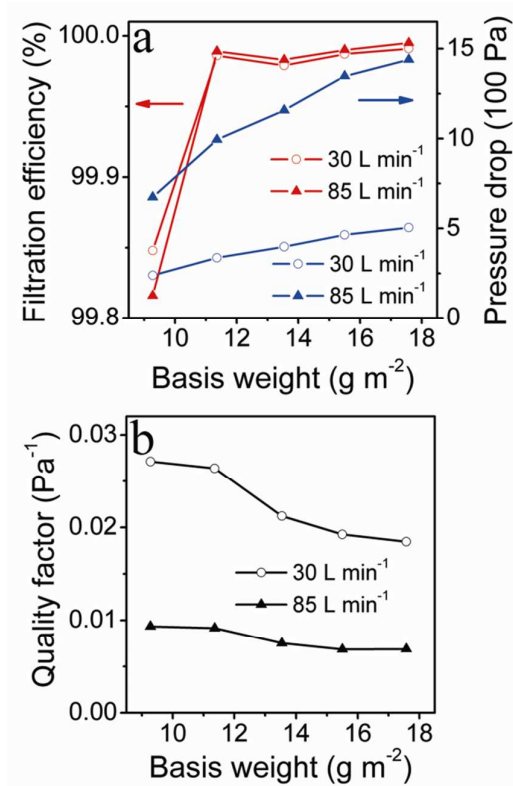
Fig. 9 Filtration performance variation *versus* the basis weight of alumina membranes calcined at 700 °C under the air flow of 30 L min^{-1} and 85 L min^{-1}. (a) Filtration efficiency and pressure drop, (b) QF values.

Fig. 9 compares the basis weight-dependent filtration performance of the alumina membrane calcined at 700 °C under the gas flow of 30 and 85 L min^{-1}, respectively. The basis weights of the membranes (9.28, 11.36, 13.54, 15.50 and 17.58 g m^{-2}) were controlled by adjusting the volume of the spinning sol (approximately 4.5, 5.5, 6.5, 7.5 and 8.5 mL). The thicknesses of the membranes are also investigated. Fig. S4 presents a typical cross-sectional view of the membrane with a basis weight of 9.28 g m^{-2}, displaying a thickness of ca.168 μm. In addition, the basis weight of the membrane has a corresponding relationship with its thickness. Specifically, the basis weights of 9.28, 11.36, 13.54, 15.50 and 17.58 g m^{-2} correspond to the thicknesses of 168, 204, 245, 281 and 317 μm. The filtration efficiencies of the membranes *versus* basis weights of 9.28, 11.36, 13.54, 15.50 and 17.58 g m^{-2} are 99.848, 99.986, 99.979, 99.987 and 99.991% at 30 L min^{-1}, while those are 99.816, 99.989, 99.983, 99.990 and 99.995% at 85 L min^{-1}. Obviously, the filtration efficiency increased rapidly at first and then reached a steady value above 99.9% when the basis weight reached 11.36 g m^{-2}. The results that are over 99.97% could meet the requirements of HEPA (high efficiency particulate air) filter standards.[43] On the other hand, the pressure drops rose steadily with the increasing of basis weight of the membrane. The pressure drop *versus* the basis weight was quite linearly, which is consistent with the previous reports.[24] The pressure drops at 30 L min^{-1} of the membranes with the basis weight of 9.28 and 11.36 g m^{-2} are respectively 239.12 and 336.14 Pa, which are relative low and favorable in practical application. Accordingly, the QF value *versus* the basis weight was shown in Fig. 8b. The QF value dropped with increasing basis weight of the membranes at both 30 and 85 L min^{-1}, which indicates that the smaller the basis weights of the membrane, the better the filtration performance. Additionally, the pressure drop increased obviously while the filtration efficiency almost unchanged when the gas flow rose from 30 L min^{-1} to 85 L min^{-1}. The increased pressure drop fits for the Darcy's law for viscous resistance, which indicates that the pressure drop increases linearly with gas flow.[46,47] According to the QF values, the membrane with lower basis weight and applied at lower gas flow possesses better filtration performance, which is cost-efficient and of great importance in practice. Therefore, the optimized thickness of the membrane is 168 μm and the corresponding basis weight is 9.28 g m^{-2}. In previous reports, the filtration performances of some other materials have been evaluated by the separation of DOP. For

example, the efficiency of processed PA6 nanofiber web was 96.8% with a resistance of 48.0 Pa at a face velocity of 5.3 cm s^{-1} (corresponding to 30 L min^{-1}),[48] and PA6/PE islands-in-the-sea bicomponent spunbond web showed a filtration efficiency of 64.1% and a resistance of 264.76 Pa at a face velocity of 5.3 cm s^{-1}.[49] Compared with these materials, the γ-alumina membrane in our study is not the one with the best filtration performance. However, these materials are polymer materials which could not be used in high-temperature circumstance. In contrast, the prepared γ-alumina membrane with good filtration property could offset this shortcoming, which could meet the requirements of HEPA (high efficiency particulate air) filter standards. Evidently, the γ-alumina membrane is a promising candidate for the high efficient fine particulate filtration in high-temperature circumstance.

Conclusions

In summary, novel self-standing γ-alumina fibrous membranes have been successfully prepared via the electrospinning method. The membranes possess good flexibility, high tensile strength and thermal stability, which is favorable in practical application. Furthermore, the membranes exhibit high filtration performance toward sub-micron aerosol particles. The filtration efficiency is 99.848% and the pressure drop is 239.12 Pa for the membrane calcined at 700 °C with a basis weight of 9.28 g m^{-2}, and the filtration efficiency could be over 99.97% when the basis weight is over 11.36 g m^{-2}. The good filtration performance of the membranes suggests that the γ-alumina membrane is of great potential to be used as high-temperature fine particulate filtration media. This work opens up the avenue of electrospinning flexible inorganic fibrous membranes for application in separation area.

Notes and references

School of Chemistry & Chemical Engineering, National Engineering Research Center for colloidal materials, Shandong University, Jinan 250100, P.R. China. Fax: +86-531-88364281; Tel: +86-531-88364280; E-mail: jiaoxl@sdu.edu.cn

1 G. Oberdörster and M. J. Utell, *Environ. Health Perspect.,* 2002, **110**, A440-A441.

2 K. Yoon, B. S. Hsiao and B. Chu, *J. Mater. Chem.* 2008, **18**, 5326-5334.

3 E. H. Wilker, M. A. Mittleman, B. A. Coull, A. Gryparis, M. L. Bots, J. Schwartz and D. Sparrow, *Environ. Health Perspect.*, 2013, **121**, 1061-1067.

4 T. Louwies, L. I. Panis, M. Kicinski, P. De Boever and T. S. Nawrot, *Environ. Health Perspect.* 2013, **121**, 1011-1016.

5 J. R. Barrett, *Environ. Health Perspect.,* 2013, **121**, A282-A282.

6 P. Dadvand, F. Figueras, X. Basagana, R. Beelen, D. Martinez, M. Cirach, A. Schembari, G. Hoek, B. Brunekreef and M. J. Nieuwenhuijsen, *Environ. Health Perspect.,* 2013, **121,** 1365-1371.

7 P. Gibson, H. Schreuder-Gibson and D. Rivin, *Colloids Surf. A: Physicochem. Eng. Asp.* 2001, **187–188**, 469-481.

8 C.-H. Hung and W. W.-F. Leung, *Sep. Purif. Technol.*, 2011, **79**, 34-42.

9 H. Ma, B. S. Hsiao and B. Chu, *Polymer*, 2011, **52**, 2594-2599.

10 B. Li and H. Cao, *J. Mater. Chem.*, 2011, **21**, 3346-3349.

11 K. Yoon, K. Kim, X. Wang, D. Fang, B. S. Hsiao and B. Chu, *Polymer*, 2006, **47**, 2434-2441.

12 R. Gopal, S. Kaur, Z. Ma, C. Chan, S. Ramakrishna and T. Matsuura, *J. Memb. Sci.*, 2006, **281**, 581-586.

13 Y. C. Ahn, S. K. Park, G. T. Kim, Y. J. Hwang, C. G. Lee, H. S. Shin and J. K. Lee, *Curr. Appl. Phys.*, 2006, **6**, 1030-1035.

14 R. Gopal, S. Kaur, C. Y. Feng, C. Chan, S. Ramakrishna, S. Tabe and T. Matsuura, *J. Memb. Sci.*, 2007, **289**, 210-219.

15 K. M. Yun, C. J. Hogan Jr, Y. Matsubayashi, M. Kawabe, F. Iskandar and K. Okuyama, *Chem. Eng. Sci.*, 2007, **62**, 4751-4759.

16 H. Ma, K. Yoon, L. Rong, Y. Mao, Z. Mo, D. Fang, Z. Hollander, J. Gaiteri, B. S. Hsiao and B. Chu, *J.*

Mater. Chem., 2010, **20**, 4692-4707.

17 Q. Zhang, J. Welch, H. Park, C.-Y. Wu, W. Sigmund and J. C. M. Marijnissen, *J. Aerosol Sci.*, 2010, **41**, 230-236.

18 W. W.-F. Leung, C.-H. Hung and P.-T. Yuen, *Sep. Purif. Technol.*, 2010, **71**, 30-37.

19 W. Sambaer, M. Zatloukal and D. Kimmer, *Chem. Eng. Sci.*, 2012, **82**, 299-311.

20 N. Wang, X. Wang, B. Ding, J. Yu and G. Sun, *J .Mater. Chem.*, 2012, **22**, 1445-1452.

21 N. Wang, A. Raza, Y. Si, J. Yu, G. Sun and B. Ding, *J. Colloid Interface Sci.*, 2013, **398**, 240-246.

22 Q. Wen, J. Di, Y. Zhao, Y. Wang, L. Jiang and J. Yu, *Chem. Sci.*, 2013, **4**, 4378-4382.

23 M. Guo, B. Ding. X. Li, X. Wang, J. Yu, and M. Wang, *J. Phys. Chem. C*, 2010, **114**, 916-921.

24 X. Mao, Y. Si, Y. Chen, L. Yang, F. Zhao, B. Ding and J. Yu, *RSC Adv.*, 2012, **2**, 12216-12223.

25 C. R. Rambo, T. Andrade, T. Fey, H. Sieber, A. E. Martinelli and P. Greil, *J. Am. Ceram. Soc.*, 2008, **91**, 852-859.

26 N. Maximous, G. Nakhla, W. Wan and K. Wong, *J. Memb. Sci.*, 2009, **341**, 67-75.

27 N. Maximous, G. Nakhla, K. Wong and W. Wan, *Sep. Purif. Technol.*, 2010, **73**, 294-301.

28 V. Su, M. Terehov and B. Clyne, *Adv. Eng. Mater.*, 2012, **14**, 1088-1096.

29 Z.-G. Zhao, N. Nagai, T. Kodaira, Y. Hukuta, K. Bando, H. Takashima and F. Mizukami, *J. Mater. Chem.*, 2011, **21**, 14984-14989.

30 N. Nagai, K. Ihara, A. Itoi, T. Kodaira, H. Takashima, Y. Hakuta, K. K. Bando, N. Itoh and F. Mizukami, *J. Mater. Chem.*, 2012, **22**, 21225-21231.

31 H. Yu, J. Guo, S. Zhu, Y. Li, Q. Zhang and M. Zhu, *Mater. Lett.*, 2012, **74**, 247-249.

32 P. Milanović, M. Dimitrijević, R. Jančić Heinemann, J. Rogan, D. B. Stojanović, A. Kojović and R. Aleksić, *Ceram. Int.*, 2013, **39**, 2131-2134.

33 A.-M. Azad, *Mater. Sci. Eng. A*, 2006, **435–436**, 468-473.

34 A. Mahapatra, B. G. Mishra and G. Hota, *Ceram. Int.*, 2011, **37**, 2329-2333.

35 Y. Wang, W. Li, X. Jiao and D. Chen, *J. Mater. Chem. A*, 2013, **1**, 10720-10726.

36 P. Zhang, D. Chen and X. Jiao, *Eur. J. Inorg.Chem.*, 2012, **26**, 4167-4173.

37 P. Zhang, D. Chen and X. Jiao, *Mater. Lett.*, 2013, **91,** 23-26.

38 J. W. Akitt and A. Farthing, *J. Chem. Soc. Dalton Trans.,* 1981, 1624-1628.

39 D. L. Guertin, S. E. Wiberley, W. H. Bauer and J. Goldenson, *J. Phys. Chem.*, 1956, **60**, 1018-1019.

40 G. B. Deacon and R. J. Phillips, *Coord. Chem. Rev.*, 1980, **33**, 227-250.

41 J. E. Crowell, J. G. Chen and J. T. Yates Jr., *J. Electron Spectrosc. Relat. Phenom.*, 1986, **39**, 97-106.

42 R. J. Jouet, A. D. Warren, D. M. Rosenberg, V. J. Bellitto, K. Park and M. R. Zachariah, *Chem.Mater.*, 2005, **17**, 2987-2996.

43 Mil.Std.282 DOP－Dept. of Defense Test Method Standard, U.S. Dept. of Defense, Washington DC **1956**.

44 G. Viswanathan, D. B. Kane and P. J. Lipowicz, *Adv. Mater.*, 2004, **16**, 2045-2049.

45 C. Y. Chen, *Chem. Rev.*, 1955, **55**, 595-623.

46 S. Whitaker, *Transp. Porous Media.* 1986, **1**, 3-25.

47 K. Onozuka, B. Ding, Y. Tsuge, T. Naka, M. Yamazaki, S. Sugi, S. Ohno, M. Yoshikawa and S. Shiratori, *Nanotechnology,* 2006, **17**, 1026-1031.

48 B. Y. Yeom, E. Shim and B. Pourdeyhimi, *Macromol. Res.*, 2010, **18**, 884-890.

49 B. Y. Yeom and B. Pourdeyhimi, *J. Mater. Sci.*, 2011, **46**, 5761-5767.

Graphical abstract

Flexible self-standing γ-alumina fibrous membranes with high efficiency filtration of sub-micron aerosols have been fabricated by electrospinning method.